THE JOURNAL OF BIOLOGICAL CHEMISTRY VOL. 290, NO. 23, pp. 14668–14678, June 5, 2015

Expression of a Catalytically Inactive Mutant Form of Glutathione Peroxidase 4 (Gpx4) Confers a Dominant-negative Effect in Male Fertility*

Received for publication, April 1, 2015, and in revised form, April 24, 2015 Published, JBC Papers in Press, April 28, 2015, DOI 10.1074/jbc.M115.656363

Irina Ingold[‡], Michaela Aichler[§], Elena Yefremova[‡], Antonella Roveri[¶], Katalin Buday[‡], Sebastian Doll[‡], Adrianne Tasdemir[‡], Nils Hoffard[‡], Wolfgang Wurst[‡‖‡‡], Axel Walch[§], Fulvio Ursini[¶], José Pedro Friedmann Angeli[‡], and Marcus Conrad[‡1]**

*From the [‡]Helmholtz Zentrum München, German Research Center for Environmental Health, Institute of Developmental Genetics, Ingolstädter Landstrassse 1, 85764 Neuherberg, Germany, [§]Research Unit Analytical Pathology, Helmholtz Zentrum München, Ingolstädter Landstrasse 1, 85764 Neuherberg, Germany, [¶]Department of Molecular Medicine, University of Padova, 35121 Padova, Italy, [‖]Deutsches Zentrum für Neurodegenerative Erkrankungen e. V. (DZNE) Standort München, Schillerstrasse 44, 80336 Munich, Germany, **Munich Cluster for Systems Neurology (SyNergy) Adolf-Butenandt-Institut Ludwig-Maximilians-Universität München, Schillerstrasse 44, 80336 Munich, Germany, and [‡‡]Technische Universität München-Weihenstephan, Lehrstuhl für Entwicklungsgenetik c/o Helmholtz Zentrum München, Ingolstädter Landstrasse 1, 85764 Neuherberg, Germany*

Background: The selenoperoxidase (Gpx4) is essential for embryogenesis, adult tissue function, and spermatogenesis.
Results: Homozygous expression of Gpx4 with a targeted substitution of selenocysteine to serine causes early embryonic death as expected but, unexpectedly, male subfertility in heterozygous mice.
Conclusion: Heterozygous expression of a catalytically inactive mutant form of Gpx4 impairs spermatogenesis.
Significance: Well-balanced expression of wild type Gpx4 is prerequisite for proper sperm development.

The selenoenzyme Gpx4 is essential for early embryogenesis and cell viability for its unique function to prevent phospholipid oxidation. Recently, the cytosolic form of Gpx4 was identified as an upstream regulator of a novel form of non-apoptotic cell death, called ferroptosis, whereas the mitochondrial isoform of Gpx4 was previously shown to be crucial for male fertility. Here, we generated and analyzed mice with a targeted mutation of the active site selenocysteine of Gpx4 (Gpx4_U46S). Mice homozygous for Gpx4_U46S died at the same embryonic stage (E7.5) as *Gpx4*$^{-/-}$ embryos as expected. Surprisingly, male mice heterozygous for Gpx4_U46S presented subfertility. Subfertility was manifested in a reduced number of litters from heterozygous breeding and an impairment of spermatozoa to fertilize oocytes *in vitro*. Morphologically, sperm isolated from heterozygous Gpx4_U46S mice revealed many structural abnormalities particularly in the spermatozoa midpiece due to improper oxidation and polymerization of sperm capsular proteins and malformation of the mitochondrial capsule surrounding and stabilizing sperm mitochondria. These findings are reminiscent of sperm isolated from selenium-deprived rodents or from mice specifically lacking mitochondrial Gpx4. Due to a strongly facilitated incorporation of Ser in the polypeptide chain as compared with selenocysteine at the UGA codon, expression of the catalytically inactive Gpx4_U46S was found to be strongly increased. Because the stability of the mitochondrial capsule of mature spermatozoa depends on the moonlighting function of Gpx4 both as an enzyme oxidizing capsular protein thiols and as a structural protein, tightly controlled expression of functional Gpx4 emerges as a key for full male fertility.

Glutathione peroxidase 4 (Gpx4[2]; previously also referred to as phospholipid hydroperoxide glutathione peroxidase) is one of eight glutathione peroxidases in mammals (1). Among the glutathione peroxidase family of proteins, Gpx4 stands out not only for its biochemical and structural traits but also for its necessity for early embryogenesis (2) and its importance for the upstream control of non-apoptotic cell death signaling (3–5). Initially discovered as a monomeric enzyme efficiently reducing hydroperoxides in lipid bilayers and complex lipoprotein particles at the expense of glutathione (GSH) or other low molecular thiol-containing compounds (6), it has become evident that Gpx4 fulfills a myriad of biochemical and cellular functions. Gpx4 controls the lipid-modulating enzymes lipoxygenase and cyclooxygenase likely through the so-called cellular peroxide tone (7), thus impinging on many inflammatory conditions and playing a superior role in cell death signaling where lipoxygenases are regarded to be involved.

Gpx4 was first considered to be an anti-apoptotic factor (8), but subsequent studies demonstrated that Gpx4 controls a caspase-independent form of non-apoptotic cell death characterized by high levels of lipid peroxidation (3). This novel form

* This work was supported in part by Deutsche Forschungsgemeinschaft (DFG) Grants CO 291/2-3 and CO 291/5-1 (to M. C.), Human Frontier Science Programme (HFSP) Grant RGP13/2014 (to M. C. and F. U.), and by a Humboldt Research Fellowship (to J. P. F. A.). This work was also funded in part by the Helmholtz Portfolio Theme "Supercomputing and Modeling for the Human Brain" (SMHB) and by the German Federal Ministry of Education and Research (BMBF) through the Integrated Network Alcoholism (Alcohol Addiction: systems-oriented approach), under the auspices of the e:Med Programme (Grant 01ZX1311G (to W. W.)).
[1] To whom correspondence should be addressed. Tel.: 49-89-3187-4608; Fax: 49-89-3187-4288; E-mail: marcus.conrad@helmholtz-muenchen.de.

[2] The abbreviations used are: Gpx4, glutathione peroxidase 4; mGpx4, mitochondrial Gpx4; Sec, selenocysteine; ES, embryonic stem; tg, transgenic; MEF, mouse embryo fibroblast.

of cell death controlled by Gpx4 was recently dubbed ferroptosis (9), relevant to cancer cell death (4), kidney dysfunction (5), and probably to many other degenerative disease conditions (3, 10–12).

Like Gpx1–3 and Gpx6, Gpx4 is a selenoprotein and harbors a selenocysteine (Sec) in its active site. Humans and mice express a total of 25 and 24 selenoproteins (Gpx6 is the only difference, being a Cys-containing variant in mice instead), respectively (13), whose functions are generally related to redox processes (14). The amino acid Sec differs from Cys only in one atom, selenium replacing sulfur. Selenium has long been regarded being an indispensable factor for male fertility (15), and a landmark study published in 1999 indeed showed that selenium in the form of Gpx4 confers the essential role in proper sperm development (16). Here, in an enzymatically inactive form Gpx4 was found to be cross-linked with other capsular proteins, presenting the major structural constituent of mitochondrial capsules that surround the mitochondria in the midpiece of mature spermatozoa and that are important for spermatozoa stability. Direct proof for the essential role of Gpx4 in male fertility was provided by specifically deleting the mitochondrial form of Gpx4 (mGpx4) in mice (17). Isolated sperm from *mGpx4*$^{-/-}$ mice phenocopied the morphological aberrations, such as bends in the midpiece, displaced heads from the midpiece, and extrusions from inner dense fibers, as had been observed much earlier for sperm that were isolated from rodents kept for several generations under severe selenium deficiency (18, 19). By contrast, mice lacking the sperm nuclei-specific form of Gpx4 (nGpx4; Ref. 20) only showed a delay in chromatin condensation (21) and an impairment in paternal chromatin decondensation (22), yet with no overt impact on overall male fertility (21).

To further challenge the importance of Sec-based catalysis of Gpx4 *in vivo*, we generated a mouse model where the catalytically important Sec was mutated to Ser. Reportedly, stable expression of a Sec/Ser mutant of Gpx4 (Gpx4_U46S) in a tamoxifen-inducible Gpx4 knock-out cell model failed to rescue cell death induced by disruption of endogenous Gpx4 expression in contrast to wild type Gpx4-expressing cells (3). As such, it was not surprising that mice expressing two Gpx4_U46S alleles died as did mice carrying a knock-out for both *Gpx4* alleles (2, 3). But surprisingly, male mice heterozygous for the Gpx4_U46S allele showed subfertility in contrast to mice heterozygous for Gpx4 (*Gpx4*$^{+/-}$), resulting from an uncontrolled increase in expression of catalytically inactive Gpx4_U46S. Our data highlight that tightly controlled Gpx4 expression is important for male fertility and that the Gpx4_U46S variant confers a dominant-negative effect over the wild type enzyme leading to impaired sperm development.

Experimental Procedures

Generation of Transgenic Mice Expressing the Serine Variant of Gpx4 (Gpx4_U46S)—For the generation of the mutant mice expressing the serine variant of Gpx4 (in the following referred to as Gpx4_U46S), the two vectors pPNT4.8 and pPNT4.10 were used (3, 17). Both plasmids were digested with SalI and SbfI, whereby the smaller fragment (4435 bp) containing the 5′ wild type sequence from pPNT4.8 (used to generate *Gpx4*$^{flox/flox}$ mice; Ref. 3) was cloned into the backbone of pPNT4.10, which was previously used to generate *mGpx4*$^{-/-}$ mice (17), thus yielding the vector pPAF-1. Next, two independent PCRs were performed using the forward AscI-fwd primer (5′-AGGAAGGCGCGCCCTCGCCGGAT-3′) and a reverse primer containing the mutation for U46S (Ser-rev, 5′-TCAGTTTTGCCGCTTTGCGAGGCCACGT-3′). For the second PCR, a forward primer containing the mutation for U46S (Ser-fwd, 5′-ACGTGGCCTCGCAAAGCGGCAAAACTGA-3′) and the SbfI-rev primer (5′-CTTCCTGGCTCCTGCAGGAAGCAAC-3′) were used to generate two PCRs products comprising either exons 2 and 3 or exons 3 and 4 of the *Gpx4* gene with an overlapping sequence in exon 3. The resulting PCR products were isolated from a low melting point agarose gel, purified, and used for an overlapping PCR using the AscI-fwd and the SbfI-rev primers. The resulting PCR product carrying the mutation was cloned into a pDrive Vector (Qiagen, Hilden, Germany). DNA isolated from pDrive was transferred into the pPAF-1 vector using AscI and SbfI (760 bp), yielding the targeting vector pPAF-1.

The targeting vector pPAF was linearized by SalI and electroporated into the embryonic stem (ES) cell line IDG3.2-rosa26. After electroporation, 150 clones were picked and analyzed for homologous insertion of the fragment into the *Gpx4* allele by long range PCR using primers oNeo_2-fwd (5′-GCGATGCCTGCTTGCCGAATATCAT-3′) and oGpx4_3-rev (5′-ACTTAGCCCATAGTCCTAAGATCAC-3′). Positive ES cell clones with homologous insertion were sequenced using primers oGpx4_mut-fwd (5′-CATGGTCTGCCTGGATAAGTACAGGT-3′) and oGpx4_mut-rev (5′-CTTGGAAGATACACTACACTGTACACTG-3′). ES cells containing the mutation were injected into blastocysts of C57BL/6 × DBA/2 F1 hybrid (BDF) mice and transferred into pseudo pregnant CD1 mice. Three chimeric mice were obtained and were backcrossed to the C57-BL/6J background for germ line transmission. Germ line transmission was confirmed by PCR in six offspring.

The genotyping of Gpx4_U46S offspring was performed by two independent PCRs specific either for the wild type (WT) allele or the transgenic (tg) allele. For the WT allele, the primers oGpx4_1-fwd (5′-GTTTAAGGATGGTGGTAACCTGCTAG-3′) and oGpx4_3-rev (5′-ACTTAGCCCATAGTCCTAAGATCAC-3′) were used to amplify a product of 256 bp in size. For the transgenic allele, primers oGpx4_2-fwd (5′-GTGGTATCATTCAGCTTTGAGAAT-3′) and oGpx4_4-rev (5′-CTCCCCTACCCGGTAGAATTAGCTTG-3′) were used yielding a product of 203 bp in size.

RNA Isolation, cDNA Synthesis, and Quantitative RT-PCR—RNA was isolated using the RNeasy Mini kit (#74104, Qiagen) according to manufacturers' instructions. For cDNA synthesis the reverse transcription system (#A3500, Promega, Mannheim, Germany) was utilized and performed as described in the manufacturers' protocol. To quantitate mRNA levels by quantitative real-time-PCR (Abiprism 7900-HT sequence detective system, Applied Biosystems, Darmstadt, Germany), a Taqman gene expression assay was performed according to manufacturers' recommendations (Applied Biosystems). For quantification of *Gpx4* mRNA levels, *Gpx4*-specific primers containing a Fam dye-labeled MGB probe (#4331182, Applied Biosystems)

were used, along with hypoxanthin-phosphoribosyltransferase-1 (*Hprt1*)-specific primers containing a Vic dye-labeled MGB-probe for the housekeeping control *Hprt1* in the same reaction (#4453320, Applied Biosystems).

Isolation of DNA from Paraffin-embedded Mouse Embryos—Heterozygous breeding for Gpx4_U46S mice was daily checked for vaginal mucous plugs. Plug-positive females were separated and sacrificed for isolation of decidua either at embryonic days E7.5 or E8.5. Decidua were fixed in 4% paraformaldehyde in PBS at 4 °C overnight followed by dehydration in an ascending series of ethanol (70, 80, 95, and 100%), incubation in xylene, and embedding in paraffin. Decidua were cut in 5-μm-thick serial sections. Sections were further processed either for hematoxylin-eosin (H&E) staining or for isolation of genomic DNA. For isolation of genomic DNA, 6–8 sections per decidua were used to scrape embryonic tissue. The pooled samples were immediately transferred into microcentrifuge tubes. 50 μl of xylene were added to the samples, and DNA was isolated using the QIAmp DNA FFPE Tissue kit (#56404, Qiagen) according to manufacturers' recommendations. 2.5 μl of the isolated DNA was directly added to a 25-μl PCR reaction mixture for genotyping the embryos with primers oGpx4_1 (fwd) and Gpx4_3 (rev) and Gpx4_2 (fwd) and Gpx4_4 (rev) for the WT and the tg alleles, respectively.

H&E Staining—Freshly dissected tissues were fixed in 4% paraformaldehyde in PBS at 4 °C overnight, dehydrated in an ascending series of ethanol (70, 80, 95, 100%), embedded in paraffin, and cut in 5-μm-thick sections. Sections were deparaffinized in xylene, hydrated in a descending ethanol series (100%, 95%, 80%), stained with Mayer's hematoxylin (Carl Roth GmbH, Karlsruhe, Germany) for 7 min, briefly washed in water, and washed by running tab water for 5 min. Sections were washed again briefly in water and stained for 3 min in 0.5% eosin Y (Sigma) containing a drop of glacial acetic acid. After a brief washing step with water, sections were dehydrated in a graded series of ethanol (70, 96, and 100%), treated with xylene, and mounted.

Isolation of DNA from Freshly Dissected Mouse Embryos—Heterozygous breeding were daily checked for vaginal mucous plugs. Plug-positive females were separated and sacrificed for embryo isolation at embryonic day E9.5. Mouse embryos were dissected in ice-cold PBS, washed twice, and transferred to microcentrifuge tubes containing 40 μl of lysis buffer (20 mM Tris-HCl, pH 8.3, 50 mM KCl, 0.45% Nonidet P-40, 0.45% Tween 20, 200 μg/ml Proteinase K). For digestion, samples were incubated for 3–4 h at 55 °C and 500 rpm in a shaker followed by a heating step at 95 °C for 10 min to inactivate Proteinase K. After heating, samples were centrifuged briefly, and 2 μl were added to a 25-μl PCR reaction mixture for genotyping with primers oGpx4_1 (fwd) and Gpx4_3 (rev) or Gpx4_2 (fwd) and Gpx4_4 (rev) for the WT and tg alleles, respectively.

Mouse Embryo Fibroblast (MEF) Cultures—For establishing Gpx4_U46S and WT control MEFs, embryos were isolated from pregnant females at E13.5 and further processed as previously described (23).

Protein Lysates from Tissues and Cells and Immunoblotting—Freshly dissected tissues were homogenized with a Eurostar RW16 stirrer in LCW lysis buffer (0.5% Triton-X-100, 0.5% sodium deoxycholate salt, 150 mM NaCl, 20 mM Tris/HCl, 10 mM EDTA, 30 mM sodium pyrophosphate, 2% protease, and 5% phosphatase inhibitor mixture (both Roche Applied Science). Cells were directly lysed in LCW lysis buffer. Cell debris was removed by centrifugation at 15,000 × *g* and 20 min at 4 °C. Protein concentration was determined using the Pierce BCA Protein Assay kit (Thermo Scientific, Bonn, Germany) according to manufacturer's protocol. Equal amounts of proteins (20 μg/lane) were separated by 12% SDS-PAGE (Bio-Rad) and blotted onto a PVDF membrane (Bio-Rad). Immunoblotting was performed with a Gpx4-specific antibody 1:1000 (#125066 Abcam, Cambridge, MA) and β-actin for quantification (#A5441, Sigma).

Immunohistochemistry—Tissues for immunohistochemical analysis were fixed in 4% paraformaldehyde in PBS at 4 °C overnight, dehydrated in an ascending series of ethanol (70, 80, 95, 100%), incubated in xylene, embedded in paraffin, and cut in 5-μm-thick sections. Sections were deparaffinized in xylene, hydrated in a descending ethanol series (100, 95, 80%), boiled in citrate buffer, pH 6, treated with 3% H_2O_2, treated with blocking solution, and incubated with Gpx4 (1:250; #125066, Abcam) or phosphohistone-3 (1:200; #9701, Cell Signaling Technologies, Danvers, MA)-specific antibodies overnight at 4 °C. Detection of primary antibody binding was performed with a biotinylated secondary antibody IgG (anti-rabbit 1:200, #BA-1000, Vector Laboratories Inc., Burlingame, CA) and an avidin-biotin-peroxidase complex (#PK-6100, Vectastain ABC kit, Vector Laboratories) to enhance the signals. 3,3′-Diaminobenzidine (#SK-4100; Vector Laboratories) staining solution was used for visualization of the staining.

Collection of Epididymal Sperm—Fresh sperm was collected from 3–8-month-old mice as described previously (17).

Protein Thiol Quantification of Epididymal Sperm by Monobromobimane Labeling—Spermatozoa were collected from caput epididymis, cauda epididymis, and vas deferens as described above. Sperm samples from WT mice (n = 9) and heterozygous Gpx4_U46S mice (n = 9) were collected by centrifugation at 5000 × *g* for 10 min at 4 °C. Collected sperm were resuspended in 1 ml of PBS and stained with 1 mM monobromobimane (#69898, Sigma) in the dark at room temperature for 30 min. Labeled sperm samples were washed twice with PBS and resuspended in 1 ml of PBS (17). Protein thiols were measured by flow cytometry (FACSCanto II, BD Biosciences) using Pacific Blue laser (452 nm).

Terminal Deoxynucleotidyltransferase dUTP Nick End Labeling (TUNEL)—TUNEL staining was performed on 5-μm thick paraffin-embedded sections as described in Conrad *et al.* (23).

Immunocytochemistry of Isolated Spermatozoa—Freshly collected sperm cells were spread on glass slides and air-dried before immunostaining. After heating at 70 °C for 1 min, spermatozoa were fixed in 2% paraformaldehyde for 10 min followed by permeabilization in 0.15% Triton X-100 (Sigma) 3 times for 5 min. Then, samples were blocked 3 times for 10 min in blocking solution containing 1% BSA and 0.15% glycine in

PBS and incubated overnight at 4 °C with a Gpx4-specific antibody (a described above) 1:100 in blocking solution. Cells were then washed in PBS for 5 min and in 0.15% Triton X-100 for 10 min and blocked again for 7 min. Sperm cells were incubated for 45 min at room temperature with the secondary antibody FITC goat anti-rabbit (#111–05-144, Jackson Immunoresearch Laboratories, West Grove, PA), which was diluted 1:200 in blocking solution. Next, sperm cells were washed twice in 0.15% Triton X-100 for 5 min and twice in PBS for 5 min at room temperature. Cells were mounted with Vectashield mounting medium containing DAPI (#H-1200, Vector Laboratories) for nuclei counterstaining. Images were acquired with an Olympus confocal microscope (Olympus IX81).

Mating Assays—Three- to six-month-old male WT mice ($n = 5$) and heterozygous Gpx4_U46S mice ($n = 5$) were mated with WT females and checked daily for vaginal plugs. At least 5 plug-positive females were collected per male, separated, and observed for offspring.

In Vitro Fertilization—The *in vitro* fertilization was conducted as described before in Schneider *et al.* (17).

Gpx4-specific Activity Assay—Gpx4-specific activity was measured in MEFs as well as in tissues derived from WT and heterozygous Gpx4_U46S animals. The activity assay was performed essentially as described previously (24).

Sperm Quality Analysis—Analysis of sperm parameters, such as motility, progressivity, and concentration was carried out as described in Schneider *et al.* (17).

Transmission Electron Microscopy—Testicular tissues were fixed in 2.5% electron microscopy grade glutaraldehyde in 0.1 M sodium cacodylate buffer, pH 7.4 (Science Services, Munich, Germany), post-fixed in 2% aqueous osmium tetraoxide, dehydrated in gradual ethanol (30–100%) and propylene oxide, embedded in Epon (Merck), and cured for 24 h at 60 °C. Semithin sections were cut and stained with toluidine blue. Ultrathin sections of 50 nm were collected onto 200 mesh copper grids stained with uranyl acetate and lead citrate before examination by transmission electron microscopy (Zeiss Libra 120 Plus, Carl Zeiss NTS GmbH, Oberkochen, Germany). Pictures were acquired using a Slow Scan CCD-camera and iTEM software (Olympus Soft Imaging Solutions, Münster, Germany).

Scanning Electron Microscopy—Specimens were fixed in (para)formaldeyde/glutaraldehyde, 3% each in 0.1 M sodium cacodylate buffer, pH 7.4 (Electron Microscopy Sciences, Hatfield, PA). Afterward, the samples were dehydrated by graded ethanol series and dried by the critical-point method using CO_2 as the transitional fluid (Polaron Critical Point Dryer). Specimens were sputter-coated with a thin layer of 7-nm platinum by a sputtering device and observed by scanning electron microscopy (JSM-6510LV; JEOL, Eching, Germany) equipped with a LaB6-emitter.

Results

Generation of Mice Expressing the U46S Mutant of Gpx4—To generate transgenic mice that express Ser instead of Sec at the catalytic site of Gpx4, we cloned a targeting vector (Fig. 1*A*) containing two point mutations in exon 3 of the *Gpx4* gene, where the opal codon UGA is localized. Homologous recombination of the targeting vector was observed in 7 out of 150 individually isolated ES cell clones that were electroporated with the targeting vector and selected with G418 and ganciclovir (Fig. 1*B*). One ES cell clone injected into BALB/C blastocysts yielded three male chimera that were subsequently backcrossed to C57BL/6J mice yielding 19 pups. Germ line transmission of the mutated Gpx4 allele was achieved in six offspring as determined by PCR analysis (Fig. 1*B*), which was further verified by sequencing of the targeted mutation (Fig. 1*C*).

Mice Homozygous for the Gpx4_U46S Variant Die during Early Embryogenesis—As homozygous offspring were never obtained from breeding of heterozygous Gpx4_U46S animals, embryos were analyzed for embryonic lethality as reported for systemic $Gpx4^{-/-}$ mice (2). Therefore, female mice from heterozygous Gpx4_U46S breeding were checked daily for vaginal mucous plugs, and pregnant animals were sacrificed at different time points post coitum (E7.5, E8.5, and E9.5; E = embryonic day) to determine their genotypes and their phenotype. Genotyping of embryos at different gestational days revealed that homozygous embryos die at E7.5-E8.5 (Table 1). At E9.5 no homozygous embryos were detectable, whereas an increased number of intrauterine resorptions and empty decidua were noticed (Table 1). Histopathological analysis of heterozygous Gpx4_U46S embryos revealed no overt abnormalities in embryonic development, whereas homozygous Gpx4_U46S embryos showed resorptions and severe abnormalities of embryonic and extraembryonic structures (Fig. 1*D*). It was not possible to unequivocally assign the three embryonic germ layers in homozygous Gpx4_U46S embryos (a characteristic of proper gastrulation), a phenotype that was already observed in constitutive *Gpx4* knock-out animals (3). From this we concluded that a homozygous Sec replacement by Ser in Gpx4 does not allow survival of mice.

Histological analysis of somatic organs (heart, lung, kidney, liver, and brain) of heterozygous Gpx4_U46S mice did not reveal any morphological aberrations (data not shown), indicating that one wild type Gpx4 allele is sufficient to allow proper development and viability of mice.

Immunoblot analysis of different tissues (heart, lung, kidney, liver, spleen, thymus, brain) consistently showed a significant up-regulation of Gpx4 protein levels in somatic tissues of heterozygous Gpx4_U46S mice (Fig. 2*A*), although there were no remarkable alterations detectable in Gpx4-specific activity in organs, such as heart, kidney, brain, and liver (Fig. 2*B*).

Next, MEFs were established from breeding of heterozygous Gpx4_U46S animals with C57BL/6J mice (Fig. 2*C*). As already observed for the different somatic tissues, Gpx4 protein levels were significantly increased in heterozygous Gpx4_U46S MEFs (Fig. 2*D*). To determine if the increased expression of Gpx4 in cells occurs at the transcriptional or translational level, quantitative real-time-PCR analysis was performed with the different cell lines. As illustrated in Fig. 2*E*, *Gpx4* mRNA levels were not significantly different from that of wild type cells, strongly suggesting that the increase of Gpx4 protein levels in heterozygous Gpx4_U46S MEFs is due to a facilitated incorporation of Ser at the respective codon in contrast to the more elaborated and less efficient incorporation of Sec at the UGA codon. Determination of Gpx4-specific activity in heterozygous MEFs showed that there was no significant change of Gpx4 activity in

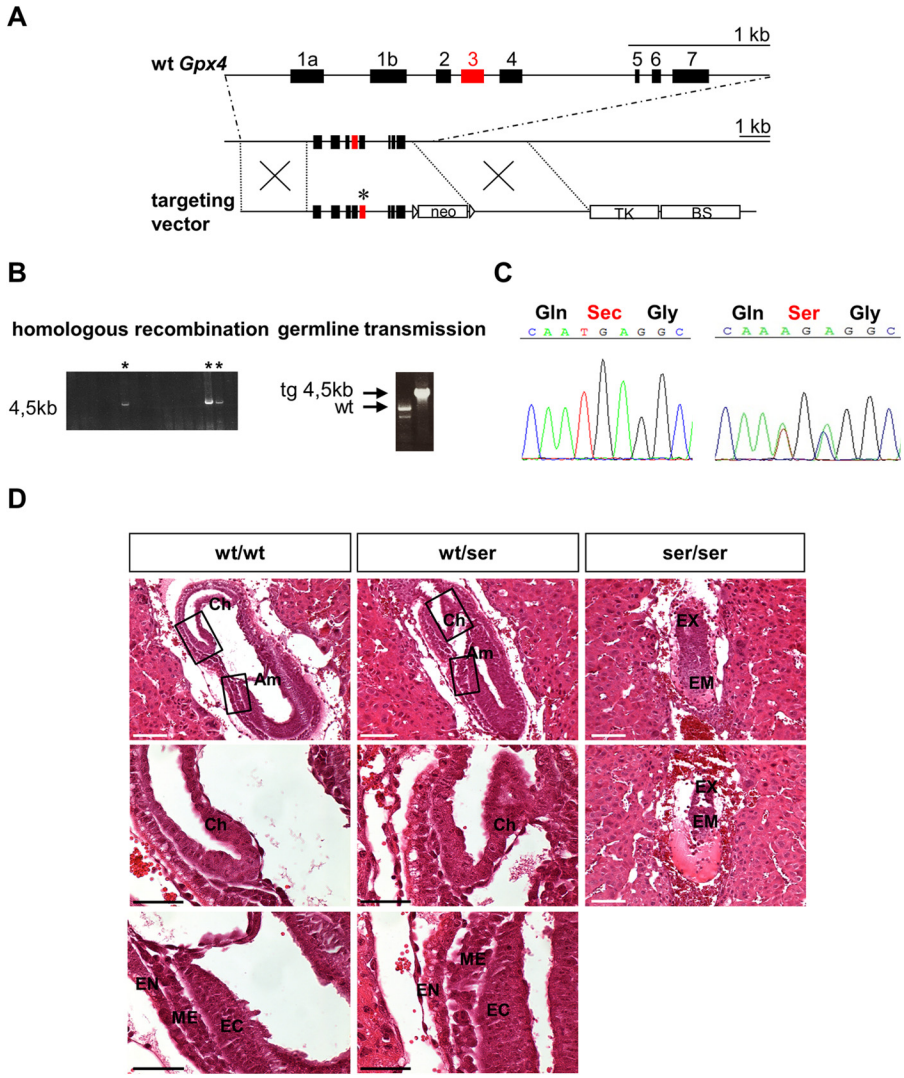

FIGURE 1. **Generation of Gpx4_U46S mice and histopathological analysis of embryos at gestational day E7.5 obtained from Gpx4_U46S heterozygous breeding.** *A*, gene targeting strategy for the site-directed mutation of Sec to Ser in Gpx4. The *upper line* depicts the WT allele of Gpx4. The *lower line* shows the targeting vector used to generate a point mutation in the active site of Gpx4, which is encoded by exon 3 (*red box*) and marked by an *asterisk*. The neomycin phosphotransferase gene (*neo*) was used for positive selection of transfected ES cells. The thymidine kinase gene (*TK*) is located downstream of the 3′ arm for homologous recombination that was utilized for negative selection (*BS*, pBluescript vector backbone). *B*, verification of homologous recombination of individual ES cell clones by long range PCR over the 3′ arm. Positive clones are marked with an *asterisk*. Germ line transmission of the targeted allele was confirmed by PCR of DNA obtained from tail biopsies. *C*, PCR amplification and sequencing of a region covering exon 3 confirmed the targeted mutation in the active site of Gpx4 (UGA → AGA) (*right panel*) in mice heterozygous for the Gpx4_U46S allele (note: in heterozygous animals a mixed sequence was detected by sequencing of tail DNA (TGA for Sec and AGC for Ser); shown is AGA, as the second A signal is slightly more prominent for the one from the TGA WT allele). *D*, H&E staining of decidua containing embryos did not reveal morphological abnormalities between WT (wt/wt) and heterozygous mutant (wt/ser) embryos. In homozygous mutant embryos (ser/ser), however, intrauterine resorptions of embryonic tissue were evident. Moreover, a clear distinction of the embryonic part in the three germinal layers was not unequivocally possible in contrast to heterozygous and WT embryos. *Am*, amnion; *CH*, chorion; *EC*, ectoderm; *EM*, embryonic tissue; *EN*, endoderm; *EX*, extraembryonic tissue; *ME*, mesoderm. *Scale bars*: *white*, 100 μm; *black*, 50 μm).

TABLE 1

Genotyping of embryos at different gestational stages

Although homozygous Gpx4_U46S embryos were readily detected at E7.5, intrauterine resorptions were frequently detected at E9.5.

Embryonic stage	wt	wt/ser	ser/ser	Resorptions
E 7.5	3 (13%)	16 (70%)	4 (17%)	0
E 8.5	6 (20%)	20 (67%)	4 (13%)	4
E 9.5	3 (17%)	15 (83%)	0 (0%)	9

heterozygous Gpx4_U46S MEFs compared with WT cells (Fig. 2*F*).

Male Gpx4_U46S Mice Are Subfertile—When setting up breeding for vaginal mucous plugs, we frequently observed that females were not pregnant despite positive plugs. Previous studies highlighted the important and multifaceted role of Gpx4 in sperm maturation (16, 17, 21, 25, 26). Therefore, we hypothesized that perturbed (*i.e.* augmented) expression of a catalytically inactive Gpx4 mutant may confer a dominant-negative effect on male fertility. To this end, test breeding was performed with male heterozygous Gpx4_U46S mice male WT mice as control. From 5 heterozygous and 5 control mice 25 plug-positive female C57BL/6J animals each were collected (Fig. 3*A*). 17 out of 25 positive plugs in the control group yielded 119 pups with litter sizes ranging from 1 to 11 pups per litter, whereas only 11 offspring (70 pups) were obtained in the heterozygous group varying between 2 and 10 pups per litter

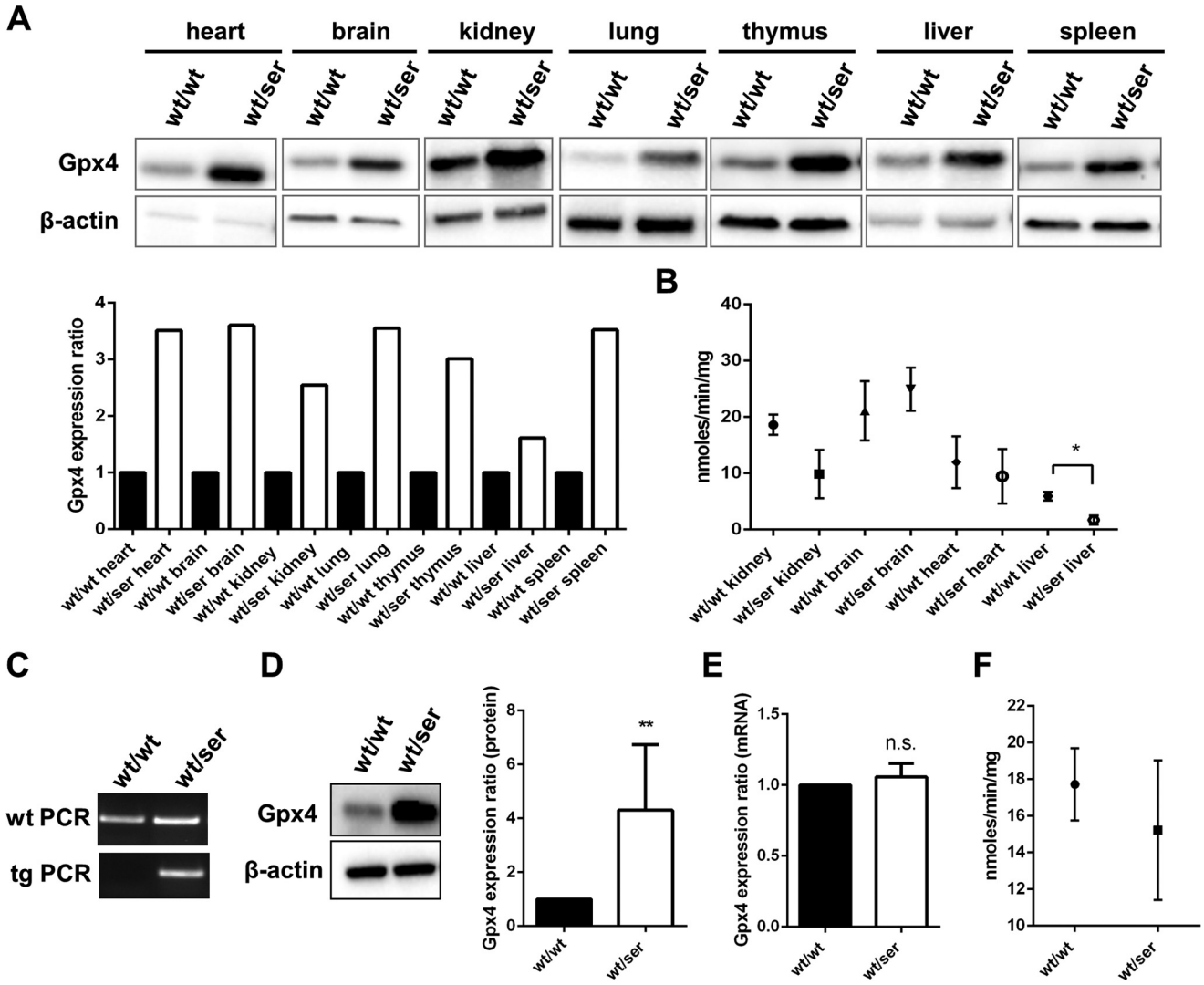

FIGURE 2. **Gpx4 expression is increased in somatic tissues and cells heterozygous for Gpx4_U46S.** *A*, Gpx4 protein levels were found to be up-regulated in all somatic tissues examined. *B*, significantly decreased levels of Gpx4-specific activities were detectable only in wt/ser livers, whereas no difference was seen in kidney, brain and heart. *C*, MEFs derived from heterozygous embryos were genotyped by two independent PCRs yielding products of 256 bp for wild type and 203 bp for heterozygous cells, respectively. *D*, despite a strong up-regulation of Gpx4 protein levels in heterozygous cells compared with wild type cells, *Gpx4* mRNA levels in these cells were found to be unaltered (*E*) (statistical analysis was conducted by using the *t* test; $p < 0.05$ (*), $p < 0.01$ (**)). *F*, Gpx4-specific activity measurement revealed no difference in Gpx4 activity in heterozygous Gpx4_U46S MEFs compared with their WT counterparts.

(Fig. 3*A*). Despite the different numbers of litters and offspring in both groups, no difference was observed in the time period between the start of breeding and until plugs were noticed (data not shown).

To further study the ability of heterozygous Gpx4_U46S sperm to fertilize oocytes and generate blastocysts *in vitro*, *in vitro* fertilization assays were conducted (Fig. 3*B*). To this end, sperm from heterozygous Gpx4_U46S mice ($n = 3$) and WT mice ($n = 3$) were incubated with 80 oocytes derived from C57BL/6J mice. In the control group, an average of 105 2-cell stage embryos developed into 20 blastocysts, whereas in the heterozygous group only 16 2-cell stage embryos were obtained of which just 2 developed to blastocysts.

Because both the *in vivo* and *in vitro* fertilization data indicated an adverse impact of the Ser variant of Gpx4 on sperm function, sperm quality parameters were assessed by using a computer-assisted semen analysis system. Although no differences were detected with regard to motility and total concentration of isolated sperm, spermatozoa from heterozygous Gpx4_U46S mice displayed a decrease in overall sperm progressivity (Fig. 3*C*). Progressivity is a routinely assessed functional parameter of isolated sperm that describes the spermatozoa's capability of rapid progressive motility, one of the key characteristics for directed movement of sperm and, thus, fertilization potential. Although less pronounced, all these data are highly reminiscent of mice specifically lacking the mitochondrial (long) form of Gpx4, which were previously shown to be infertile (17).

(Immuno)histopathological Analysis of Gpx4_U46S Mutant Mice—For the observed impairment of sperm quality and fertility of heterozygous Gpx4_U46S males, we next analyzed testicular and epididymal tissues and spermatozoa for morphological alterations or changes in Gpx4 expression. H&E staining of testis, caput epididymis, and cauda epididymis did not reveal

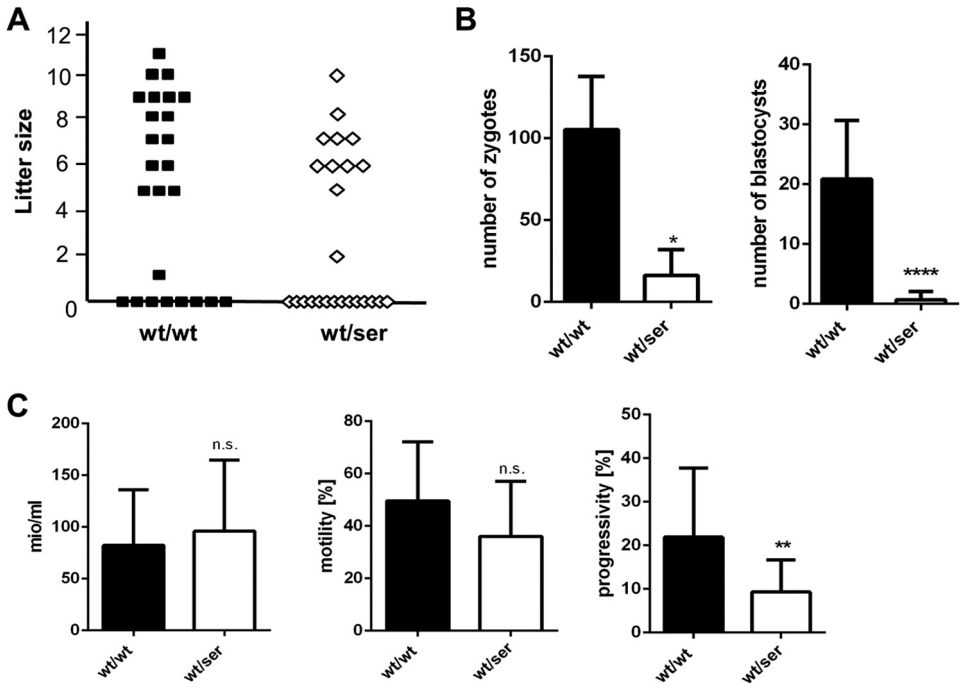

FIGURE 3. **Heterozygous Gpx4_U46S mice are subfertile.** *A*, test breeding of male WT (wt/wt) and heterozygous Gpx4_U46S (wt/ser) mice with C57BL/6J yielded a total of 17 litters with a total number of 119 offspring in the WT group and 11 litters with a total number of 70 offspring in the heterozygous Gpx4_U46S group ($n = 5$ males each genotype). *B*, *in vitro* fertilization with sperm isolated from wild type and heterozygous animals showed a significant difference in the number of zygotes (pro-nuclei stage) and developed blastocysts ($n = 3$ each genotype) obtained from the different genotypes. *C*, sperm quality analysis showed no difference in total sperm concentration and motility between wild type and heterozygous spermatozoa, whereas progressivity was found to be impaired in sperm isolated from heterozygous donors ($n = 9$ wt/wt; $n = 17$ wt/ser). Statistical analysis was performed by using *t* test $p < 0.05$ (*), $p < 0.01$ (**), and $p < 0.0001$ (****). *n.s.*, not significant.

any overt histological abnormalities (Fig. 4*A*). Likewise, we did not detect any differences in the numbers of dying cells as determined by TUNEL staining in testicular and epididymal tissues of heterozygous Gpx4_U46S mice compared with WT mice (data not shown).

Western blot analysis (Fig. 4*B*) of testicular and epididymal tissues and immunohistochemical analysis of testicular tissue showed a higher expression of Gpx4 protein levels as already observed for somatic tissue (see Fig. 2*A*), most likely resulting from an increased translation efficiency of the Gpx4_U46S mutant form as suggested from the quantitative real-time-PCR analysis of testicular tissue (Fig. 4*C*). Gpx4-specific activity tended to be decreased in testicular tissue of heterozygous males (Fig. 4*D*). Immunocytochemical staining of whole-mount spermatozoa also revealed an elevated expression of Gpx4 particularly in the midpiece and the head of isolated spermatozoa (Fig. 4*E*), where the mitochondrial and the nuclear isoforms of Gpx4 are localized (17, 20).

Severe Morphological Alterations of Sperm Derived from Gpx4_U46S Mice—When the immunocytochemical studies were performed, morphological abnormalities in isolated sperm cells were noticeable, which were mainly confined to the midpiece of mature spermatozoa. Therefore, we extended these investigations and performed ultrastructural analyses of epididymal sperm. By transmission electron microscopy swollen mitochondria surrounding the axoneme in late stage spermatids were detected in samples from heterozygous Gpx4_U46S mutant mice (Fig. 5*A*). Scanning electron microscopy of isolated spermatozoa confirmed many morphological aberrations particularly in the midpiece and midpiece-principal piece junction (Fig. 5*B*). Aberrations included bends mainly at the midpiece-principal piece junction, irregularly aligned mitochondria, and protrusions of outer dense fibers. Notably, all these morphological aberrations were reported in spermatozoa from rodents that had been kept for several generations on a selenium-deprived diet (18, 19) and in animals specifically lacking mGpx4 (17).

Higher Levels of Free Thiols in U46S Sperm—From the *in vitro* and *in vivo* functional data and the structural aberrations observed in Gpx4_U46S sperm, we hypothesized that increased expression of catalytically inactive Gpx4 confers a dominant-negative role in male fertility. This effect might be brought about by the vitally important role of Gpx4 as thiol-peroxidizing enzyme in cross-linking mitochondrial capsular proteins in the sperm by disulfide bridges (25), thus conferring full rigidity and spermatozoa midpiece stability (27).

We thus assessed the overall free thiol content by monobromobimane labeling of free thiols in sperm cells isolated from heterozygous Gpx4_U46S mutant mice ($n = 9$) and WT ($n = 9$) littermates. We directly compared spermatozoa from caput epididymis and cauda epididymis. It is well known that during epididymal transit, spermatozoa undergo massive oxidation in sperm proteins in order to fully stabilize sperm structures by disulfide bridges. These oxidative steps are facilitated, as during the final steps of spermiogenesis the majority of intracellular glutathione (GSH) is lost in maturing sperm cells (28). As illustrated in Fig. 6, flow cytometry analysis of sperm cells of Gpx4_U46S mice revealed a significantly increased fluores-

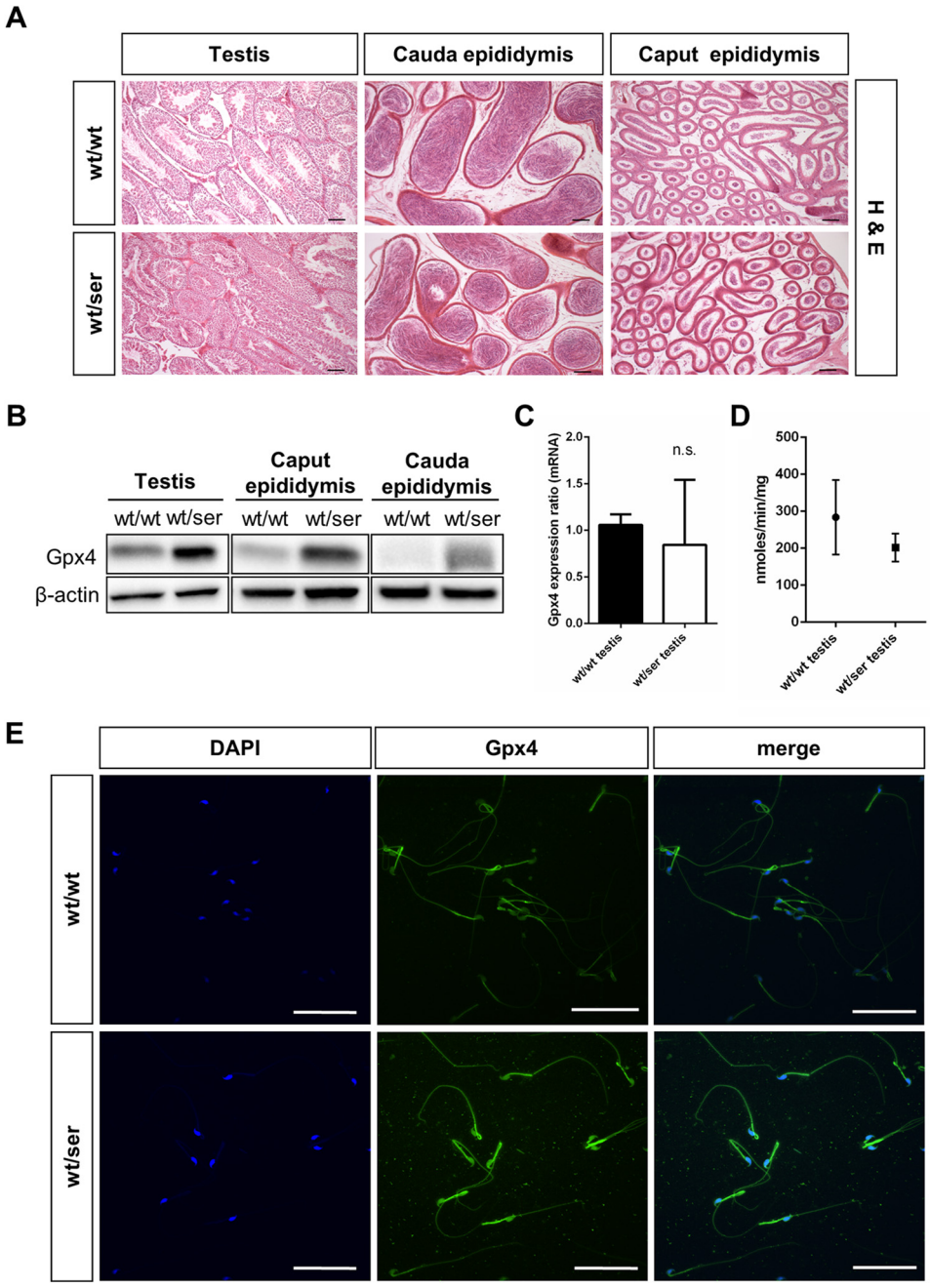

FIGURE 4. **Immunohistological analysis of germinal epithelium and isolated spermatozoa.** *A*, H&E analysis of testis and epididymis did not show any overt differences between wild type and homozygous tissues (*scale bar* = 100 μm). *B*, as observed for somatic tissues, Gpx4 immunoblotting in testis and epididymal tissue presented a stronger Gpx4 signal in heterozygous samples compared with wild type tissue. *C*, quantitative RT-PCR of *Gpx4* levels in testicular tissue did not show a statistically significant difference between wild type and heterozygous testis. *n.s.*, not significant. *D*, measurement of Gpx4-specific activity revealed a tendency toward decreased activity, but it did not reach statistical significance in heterozygous testicular tissue. *E*, whole mounts staining of epididymal spermatozoa revealed an increase in Gpx4 immunoreactivity (*green*) in heterozygous sperm that was mainly confined to the midpiece and the head region of sperm. Sperm nuclei were additionally counterstained with DAPI (*scale bar* = 50 μm).

cence signal in cauda epididymis compared with sperm from WT mice (Fig. 6, *A* and *B*). This indicates that sperm protein thiols from Gpx4_U46S mice were consistently found in a more reduced state, thus contributing to impaired formation of mitochondrial capsules, as already observed in the ultrastructural analyses (see Fig. 5).

Discussion

Gpx4 belongs to a discrete set of mammalian proteins that harbor one or several Sec residues in their active site (14). Among the family of selenoproteins in mammals (24 in mice and 25 in man), Gpx4 appears to be the most limiting enzyme, as the gene knock-out in mice leads to early embryonic lethality around gastrulation (~E7.5) (2), a time point that is fairly close to the stage when Sec-specific tRNA knock-out mice die (E6.5) due to loss of expression of all selenoproteins simultaneously (29). To address the importance of selenothiol-mediated Gpx4 catalysis in one of the most important mammalian selenoproteins, we have thus generated mice with a targeted mutation in the catalytic site of Gpx4, Ser replacing Sec. Mice

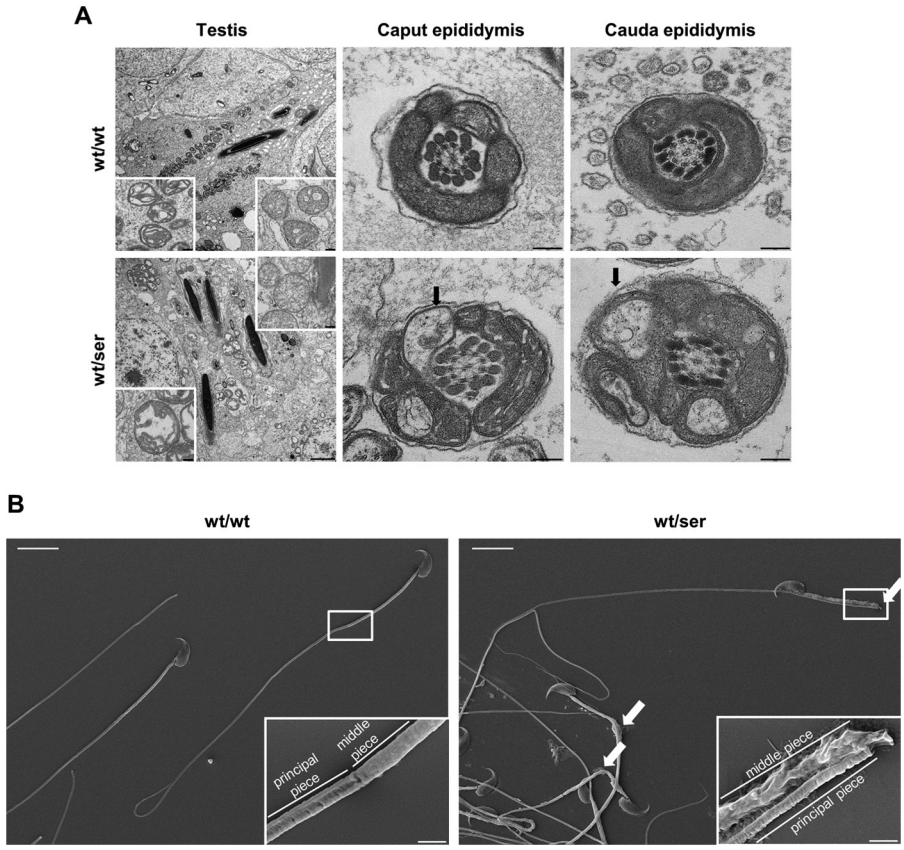

FIGURE 5. **Severe morphological alterations in the midpiece of developing and mature sperm.** *A*, transmission electron microscopy showed an increase in swollen mitochondria in late spermatids (testis) and epididymal spermatozoa (*arrows*). *B*, scanning electron microscopy of isolated sperm revealed severe morphological aberrations in the midpiece and the midpiece-principal piece junction of heterozygous spermatozoa (*scale bar*: *A*, 2 μm, insets = 200 nm; *B*, 10 μm, insets = 1 μm).

homozygous for the U46S mutation die as $Gpx4^{-/-}$ knock-out mice, whereas heterozygous Gpx4_U46S mice develop normally and do not present any overt phenotype. These data are in line with a recent report indicating that mice expressing a U46A variant of Gpx4 die around the same embryonic stage as reported here (30). These and our findings are not surprising as it was previously demonstrated that ectopic expression of the catalytically inactive U46S variant in tamoxifen-inducible Gpx4 knock-out cells failed to suppress cell death induced by Gpx4 ablation (31). Hence, this supports the notion that the survival function of Gpx4 is conferred by its peroxidase activity mediated through Sec.

Unlike the study with heterozygous Gpx4_U46A mice, where no impact of heterozygosity on male fertility has been indicated (30), we observed an impairment of male fertility of heterozygous Gpx4_U46S mice. This was manifested by reduced numbers of litters from heterozygous Gpx4_U46S males, a strong impairment of the *in vitro* fertilizing capability of sperm derived from heterozygous Gpx4_U46S mice, and many morphological aberrations particularly in the spermatozoon midpiece. This phenotype, although less pronounced, strongly resembles mice specifically lacking mGpx4 (17). Mice homozygous knock-out for mGpx4 are fully viable, but male mice were found to be infertile. Defects in the midpiece of spermatozoa from these mice phenocopied the defects observed in sperm isolated from rodents kept on a selenium-deprived diet for several generations (18, 19). Here, mGpx4 not only acts as the major structural protein interacting with capsular proteins (16) but also as a thiol peroxidase cross-linking capsular protein, including itself, via disulfide bridges, thus, conferring full midpiece stability. When no further thiols are present, mGpx4 becomes cross-linked via disulfide and selenyl-sulfide bridges with other proteins (25).

As total Gpx4 protein levels of heterozygous Gpx4_U46S males were found to be strongly augmented in almost all tissues examined including epididymis, we hypothesized that the increase of catalytically inactive Gpx4 confers a dominant-negative effect in proper sperm capsule formation. This was corroborated by the fact that staining of sperm cells against free thiols with monobromobimane showed that there was indeed an increase in free reduced thiols in the cauda epididymis compared with WT sperm (Fig. 6). Although this increase did not interfere with proliferation of somatic cells and did not adversely impact on normal embryo development and tissue homeostasis, this dominant-negative effect only surfaced in proper sperm capsule formation. Thereby, it is conceivable that the abundance of too high levels of catalytically inactive Gpx4_U46S interferes with the reported essential role of WT Gpx4 as a thiol peroxidase by cross-linking sperm proteins through disulfide (and selenyl-sulfide) bridges (25, 27). Although all of the eight remaining Cys residues in Gpx4 are still present in the Gpx4_U46S mutant protein, which are still able to be used by the WT Gpx4 enzyme for forming intra- and

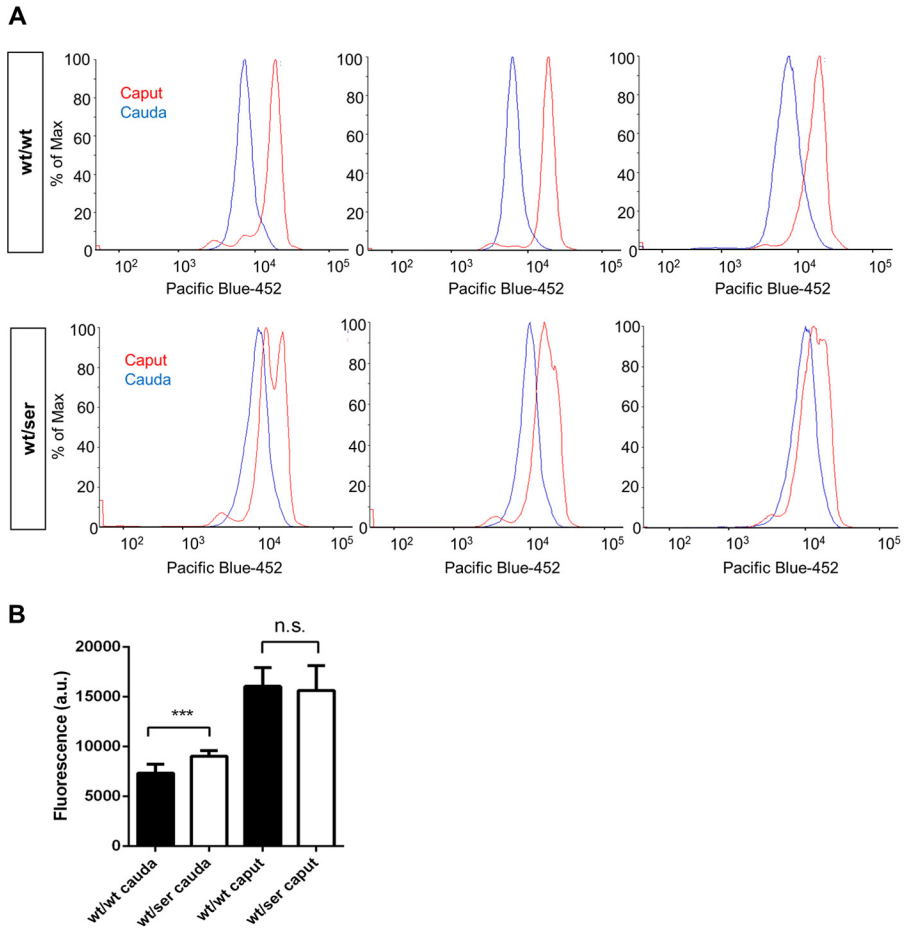

FIGURE 6. **Higher levels of free thiols in cauda epididymis spermatozoa from heterozygous Gpx4_U46S mice.** *A*, monobromobimane-labeled spermatozoa revealed an augmented fluorescence intensity signal in heterozygous animals in comparison to WT samples, whereas no detectable difference in the free thiol content was observed in spermatozoa derived from caput epididymis of both genotypes. *B*, a quantitative evaluation of the flow cytometry data in *A* revealed a statistically significant difference in free thiols between sperm samples only in those isolated from cauda epididymis (statistical analysis was conducted using *t* test; $p < 0.001$ (***)). *a.u.*, arbitrary units. *n.s.*, not significant.

intermolecular (selenyl)disulfide bridges with WT Gpx4 and other capsular proteins including sperm mitochondria-associated cysteine-rich protein (SMCP) and different types of keratins, an imbalance in expression between the WT and the mutant enzyme most likely favors incomplete oxidation of capsular proteins as also detected by monobromobimane labeling. Hence, this underlines the importance of selenium incorporation in Gpx4 for male fertility.

Despite the observed increase in Gpx4 expression levels in all tissues examined, no differences of *Gpx4* mRNA levels were detectable in the respective tissues. It is thus reasonable to assume that incorporation of Ser at its cognate codon is greatly facilitated compared with the co-translational decoding of the UGA codon. In a previous study aiming to address the efficiency and kinetics of UGA decoding it was demonstrated that Sec incorporation at the UGA codon in *Escherichia coli* is in the range of 3–5% when compared with Ser incorporation (32). Therefore, it is conceivable that "overproduction" of the U46S variant severely perturbs disulfide cross-linking of Gpx4 WT protein. In this context it is noteworthy that transgenic mice expressing active mGpx4 under the control of the synaptonemal complex protein 1 promoter leading to mGpx4 expression already at the diplotene-zygotene stage during meiosis presented reduced male fertility manifested by increased sperm cell death and reduced litter size (33).

Hence, one can conclude that Gpx4 represents a very peculiar case where the same protein functions both as an enzyme and a substrate. As the enzymatic activity was not found to be strongly changed in testis from heterozygous Gpx4_U46S mice, the excess of substrate likely alters the optimal cross-linking as the enzyme becomes inactive in its cross-linked form (16), whereas at the same time an excess of reduced thiols remains, leaving sperm capsular proteins only partially polymerized. In conclusion, data presented here strongly suggest that well balanced expression of functional Gpx4 emerges as prerequisite for full male fertility.

Acknowledgments—We thank Sonja Gürster and Susanne Cornfine from JEOL.

References

1. Brigelius-Flohé, R., and Maiorino, M. (2013) Glutathione peroxidases. *Biochim. Biophys. Acta* **1830,** 3289–3303
2. Yant, L. J., Ran, Q., Rao, L., Van Remmen, H., Shibatani, T., Belter, J. G., Motta, L., Richardson, A., and Prolla, T. A. (2003) The selenoprotein GPX4 is essential for mouse development and protects from radiation and

oxidative damage insults. *Free Radic. Biol. Med.* **34,** 496–502
3. Seiler, A., Schneider, M., Förster, H., Roth, S., Wirth, E. K., Culmsee, C., Plesnila, N., Kremmer, E., Rådmark, O., Wurst, W., Bornkamm, G. W., Schweizer, U., and Conrad, M. (2008) Glutathione peroxidase 4 senses and translates oxidative stress into 12/15-lipoxygenase dependent- and AIF-mediated cell death. *Cell Metab.* **8,** 237–248
4. Yang, W. S., SriRamaratnam, R., Welsch, M. E., Shimada, K., Skouta, R., Viswanathan, V. S., Cheah, J. H., Clemons, P. A., Shamji, A. F., Clish, C. B., Brown, L. M., Girotti, A. W., Cornish, V. W., Schreiber, S. L., and Stockwell, B. R. (2014) Regulation of ferroptotic cancer cell death by GPX4. *Cell* **156,** 317–331
5. Friedmann Angeli, J. P., Schneider, M., Proneth, B., Tyurina, Y. Y., Tyurin, V. A., Hammond, V. J., Herbach, N., Aichler, M., Walch, A., Eggenhofer, E., Basavarajappa, D., Rådmark, O., Kobayashi, S., Seibt, T., Beck, H., Neff, F., Esposito, I., Wanke, R., Förster, H., Yefremova, O., Heinrichmeyer, M., Bornkamm, G. W., Geissler, E. K., Thomas, S. B., Stockwell, B. R., O'Donnell, V. B., Kagan, V. E., Schick, J. A., and Conrad, M. (2014) Inactivation of the ferroptosis regulator Gpx4 triggers acute renal failure in mice. *Nat. Cell Biol.* **16,** 1180–1191
6. Ursini, F., Maiorino, M., Valente, M., Ferri, L., and Gregolin, C. (1982) Purification from pig liver of a protein which protects liposomes and biomembranes from peroxidative degradation and exhibits glutathione peroxidase activity on phosphatidylcholine hydroperoxides. *Biochim. Biophys. Acta* **710,** 197–211
7. Conrad, M., Schneider, M., Seiler, A., and Bornkamm, G. W. (2007) Physiological role of phospholipid hydroperoxide glutathione peroxidase in mammals. *Biol. Chem.* **388,** 1019–1025
8. Nomura, K., Imai, H., Koumura, T., Arai, M., and Nakagawa, Y. (1999) Mitochondrial phospholipid hydroperoxide glutathione peroxidase suppresses apoptosis mediated by a mitochondrial death pathway. *J. Biol. Chem.* **274,** 29294–29302
9. Dixon, S. J., Lemberg, K. M., Lamprecht, M. R., Skouta, R., Zaitsev, E. M., Gleason, C. E., Patel, D. N., Bauer, A. J., Cantley, A. M., Yang, W. S., Morrison, B., 3rd, and Stockwell, B. R. (2012) Ferroptosis: an iron-dependent form of nonapoptotic cell death. *Cell* **149,** 1060–1072
10. Wirth, E. K., Conrad, M., Winterer, J., Wozny, C., Carlson, B. A., Roth, S., Schmitz, D., Bornkamm, G. W., Coppola, V., Tessarollo, L., Schomburg, L., Köhrle, J., Hatfield, D. L., and Schweizer, U. (2010) Neuronal selenoprotein expression is required for interneuron development and prevents seizures and neurodegeneration. *FASEB J.* **24,** 844–852
11. Ueta, T., Inoue, T., Furukawa, T., Tamaki, Y., Nakagawa, Y., Imai, H., and Yanagi, Y. (2012) Glutathione peroxidase 4 is required for maturation of photoreceptor cells. *J. Biol. Chem.* **287,** 7675–7682
12. Wortmann, M., Schneider, M., Pircher, J., Hellfritsch, J., Aichler, M., Vegi, N., Kölle, P., Kuhlencordt, P., Walch, A., Pohl, U., Bornkamm, G. W., Conrad, M., and Beck, H. (2013) Combined deficiency in glutathione peroxidase 4 and vitamin E causes multiorgan thrombus formation and early death in mice. *Circ. Res.* **113,** 408–417
13. Kryukov, G. V., Castellano, S., Novoselov, S. V., Lobanov, A. V., Zehtab, O., Guigó, R., and Gladyshev, V. N. (2003) Characterization of mammalian selenoproteomes. *Science* **300,** 1439–1443
14. Hatfield, D. L., Tsuji, P. A., Carlson, B. A., and Gladyshev, V. N. (2014) Selenium and selenocysteine: roles in cancer, health, and development. *Trends Biochem. Sci.* **39,** 112–120
15. Wu, S. H., Oldfield, J. E., Whanger, P. D., and Weswig, P. H. (1973) Effect of selenium, vitamin E, and antioxidants on testicular function in rats. *Biol. Reprod.* **8,** 625–629
16. Ursini, F., Heim, S., Kiess, M., Maiorino, M., Roveri, A., Wissing, J., and Flohé, L. (1999) Dual function of the selenoprotein PHGPx during sperm maturation. *Science* **285,** 1393–1396
17. Schneider, M., Förster, H., Boersma, A., Seiler, A., Wehnes, H., Sinowatz, F., Neumüller, C., Deutsch, M. J., Walch, A., Hrabé de Angelis, M., Wurst, W., Ursini, F., Roveri, A., Maleszewski, M., Maiorino, M., and Conrad, M. (2009) Mitochondrial glutathione peroxidase 4 disruption causes male infertility. *FASEB J.* **23,** 3233–3242
18. Wallace, E., Calvin, H. I., and Cooper, G. W. (1983) Progressive defects observed in mouse sperm during the course of three generations of selenium deficiency. *Gamete Res.* **7,** 377–387
19. Wallace E., Cooper, G. W., and Calvin H. L. (1983) Effects of selenium deficiency on the shape and arrangement of rodent sperm mitochondria. *Gamete Res.* **7,** 389–399
20. Pfeifer, H., Conrad, M., Roethlein, D., Kyriakopoulos, A., Brielmeier, M., Bornkamm, G. W., and Behne, D. (2001) Identification of a specific sperm nuclei selenoenzyme necessary for protamine thiol cross-linking during sperm maturation. *FASEB J.* **15,** 1236–1238
21. Conrad, M., Moreno, S. G., Sinowatz, F., Ursini, F., Kölle, S., Roveri, A., Brielmeier, M., Wurst, W., Maiorino, M., and Bornkamm, G. W. (2005) The nuclear form of phospholipid hydroperoxide glutathione peroxidase is a protein thiol peroxidase contributing to sperm chromatin stability. *Mol. Cell. Biol.* **25,** 7637–7644
22. Puglisi, R., Maccari, I., Pipolo, S., Conrad, M., Mangia, F., and Boitani, C. (2012) The nuclear form of glutathione peroxidase 4 is associated with sperm nuclear matrix and is required for proper paternal chromatin decondensation at fertilization. *J. Cell. Physiol.* **227,** 1420–1427
23. Conrad, M., Jakupoglu, C., Moreno, S. G., Lippl, S., Banjac, A., Schneider, M., Beck, H., Hatzopoulos, A. K., Just, U., Sinowatz, F., Schmahl, W., Chien, K. R., Wurst, W., Bornkamm, G. W., and Brielmeier, M. (2004) Essential role for mitochondrial thioredoxin reductase in hematopoiesis, heart development, and heart function. *Mol. Cell. Biol.* **24,** 9414–9423
24. Roveri, A., Maiorino, M., and Ursini, F. (1994) Enzymatic and immunological measurements of soluble and membrane-bound phospholipid-hydroperoxide glutathione peroxidase. *Methods Enzymol.* **233,** 202–212
25. Maiorino, M., Roveri, A., Benazzi, L., Bosello, V., Mauri, P., Toppo, S., Tosatto, S. C., and Ursini, F. (2005) Functional interaction of phospholipid hydroperoxide glutathione peroxidase with sperm mitochondrion-associated cysteine-rich protein discloses the adjacent cysteine motif as a new substrate of the selenoperoxidase. *J. Biol. Chem.* **280,** 38395–38402
26. Imai, H., Hakkaku, N., Iwamoto, R., Suzuki, J., Suzuki, T., Tajima, Y., Konishi, K., Minami, S., Ichinose, S., Ishizaka, K., Shioda, S., Arata, S., Nishimura, M., Naito, S., and Nakagawa, Y. (2009) Depletion of selenoprotein GPx4 in spermatocytes causes male infertility in mice. *J. Biol. Chem.* **284,** 32522–32532
27. Conrad, M., Ingold, I., Buday, K., Kobayashi, S., and Angeli, J. P. (2014) ROS, thiols and thiol-regulating systems in male gametogenesis. *Biochim. Biophys. Acta* 10.1016/j.bbagen.2014.10.020
28. Shalgi, R., Seligman, J., and Kosower, N. S. (1989) Dynamics of the thiol status of rat spermatozoa during maturation: analysis with the fluorescent labeling agent monobromobimane. *Biol. Reprod.* **40,** 1037–1045
29. Bösl, M. R., Takaku, K., Oshima, M., Nishimura, S., and Taketo, M. M. (1997) Early embryonic lethality caused by targeted disruption of the mouse selenocysteine tRNA gene (Trsp). *Proc. Natl. Acad. Sci. U.S.A.* **94,** 5531–5534
30. Brütsch, S. H., Wang, C. C., Li, L., Stender, H., Neziroglu, N., Richter, C., Kuhn, H., and Borchert, A. (2015) Expression of inactive glutathione peroxidase 4 leads to embryonic lethality, and inactivation of the alox15 gene does not rescue such knock-in mice. *Antioxid. Redox Signal.* **22,** 281–293
31. Mannes, A. M., Seiler, A., Bosello, V., Maiorino, M., and Conrad, M. (2011) Cysteine mutant of mammalian GPx4 rescues cell death induced by disruption of the wild-type selenoenzyme. *FASEB J.* **25,** 2135–2144
32. Suppmann, S., Persson, B. C., and Böck, A. (1999) Dynamics and efficiency in vivo of UGA-directed selenocysteine insertion at the ribosome. *EMBO J.* **18,** 2284–2293
33. Puglisi, R., Bevilacqua, A., Carlomagno, G., Lenzi, A., Gandini, L., Stefanini, M., Mangia, F., and Boitani, C. (2007) Mice overexpressing the mitochondrial phospholipid hydroperoxide glutathione peroxidase in male germ cells show abnormal spermatogenesis and reduced fertility. *Endocrinology* **148,** 4302–4309

Enzymology:

Expression of a Catalytically Inactive Mutant Form of Glutathione Peroxidase 4 (Gpx4) Confers a Dominant-negative Effect in Male Fertility

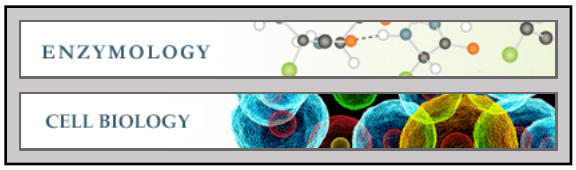

Irina Ingold, Michaela Aichler, Elena Yefremova, Antonella Roveri, Katalin Buday, Sebastian Doll, Adrianne Tasdemir, Nils Hoffard, Wolfgang Wurst, Axel Walch, Fulvio Ursini, José Pedro Friedmann Angeli and Marcus Conrad

J. Biol. Chem. 2015, 290:14668-14678.
doi: 10.1074/jbc.M115.656363 originally published online April 28, 2015
